optica

Polarization-assisted amplitude gating as a route to tunable, high-contrast attosecond pulses

Henry Timmers,[1,†,4] Mazyar Sabbar,[1,†] Johannes Hellwagner,[1] Yuki Kobayashi,[1] Daniel M. Neumark,[1,2,5] and Stephen R. Leone[1,2,3,*]

[1]Department of Chemistry, University of California, Berkeley, California 94720, USA
[2]Chemical Sciences Division, Lawrence Berkeley National Laboratory, Berkeley, California 94720, USA
[3]Department of Physics, University of California, Berkeley, California 94720, USA
[4]e-mail: htimmers@berkeley.edu
[5]e-mail: dneumark@berkeley.edu
*Corresponding author: srl@berkeley.edu

Received 23 March 2016; revised 13 May 2016; accepted 18 May 2016 (Doc. ID 261676); published 28 June 2016

Attosecond spectroscopy is a powerful technique for probing electron dynamics in fundamental systems. However, extending this method to cover a wide range of element-specific, core-hole transitions requires the availability of broadly tunable attosecond pulses. In this Letter, we present a new method for generating high-flux, high-contrast single attosecond pulses tunable across the range of 50–120 eV. The method is referred to as a Polarization ASSisted Amplitude GatE (PASSAGE) and uses a few-cycle driving pulse along with a partial polarization gate to extend the bandwidth of high harmonic emission in the temporally isolated, cut-off portion of the spectrum. The simplicity of this technique will help pave the way for implementing attosecond core–hole spectroscopy to probe more complex reactions and bring attosecond science into a multidisciplinary setting.

OCIS codes: (320.7150) Ultrafast spectroscopy; (320.7110) Ultrafast nonlinear optics; (340.7480) X-rays, soft x-rays, extreme ultraviolet (EUV).

http://dx.doi.org/10.1364/OPTICA.3.000707

Attosecond pulses in the extreme ultraviolet (XUV) are generated through the highly nonlinear process of high harmonic generation (HHG) [1]. A near-infrared (NIR), femtosecond pulse undergoes a non-perturbative interaction with a noble gas medium, leading to the generation of high-order harmonics of the fundamental NIR field. The harmonics are emitted in attosecond bursts that occur every half laser cycle. While HHG offers a simple means of generating a train of these attosecond pulses, isolating a single attosecond pulse (SAP) is significantly more difficult. Only a handful of methods exist that have demonstrated the ability to generate SAPs. These methods include amplitude gating [2], polarization gating (PG) [3–5], double optical gating (DOG) [6], generalized DOG [7], ionization gating [8,9], and the attosecond lighthouse effect [10]. Of these methods, the most versatile have been amplitude gating, PG, and DOG. The method of amplitude gating uses few-cycle femtosecond pulses as a driver for HHG. Since the electric field amplitude changes dramatically from one half-cycle to the next, the most energetic XUV photons originate from the HHG emission corresponding to the most intense half-cycle [2]. This creates a quasi-continuum in the most energetic portion of the HHG spectrum, referred to as the cut-off spectrum. On the other hand, PG and DOG take advantage of the extreme ellipticity dependence of HHG by tailoring the polarization of the driving pulse such that it is linearly polarized for a fraction of an optical cycle [3], leading to isolated attosecond emission.

In this report, we introduce a new technique for generating a SAP. The method provides an extension to amplitude gating by incorporating a partial polarization gate to suppress HHG emission from half-cycles adjacent to the most intense half-cycle of the driving laser field. We refer to the method as a Polarization ASSisted Amplitude GatE (PASSAGE). The optical layout for PASSAGE is shown in Fig. 1(a). The layout is similar to PG and consists of only two optical elements. The first optic is a $L = 85$ μm quartz plate with an optical axis parallel to the surface of the plate and placed at an angle of 45° with respect to the input polarization. The thickness of this plate is chosen to correspond to the first-order full waveplate thickness of quartz at 780 nm and generates two time-delayed, orthogonally polarized pulses. The second optic is a zeroth-order $\lambda/4$ plate that converts the orthogonally polarized pulses to counterrotating, elliptically polarized pulses. The overlap of these pulses is determined by the group delay introduced by the first quartz plate, which sets the duration of the linear polarization gate. For full PG, a linear gate of $\leq$0.5 optical cycles (o.c.) is used to isolate a SAP, corresponding to a thickness of $L = 180$ μm. For PASSAGE, only a weak polarization gate is required to isolate the cut-off spectrum. For pulse durations greater than 3.5 fs, the $L = 85$ μm plate gives rise to a linear polarization gate >0.5 o.c. Figure 1(b) shows the time-dependent ellipticity created by the PASSAGE configuration for a 5 fs driving pulse duration. The linear gate width for this configuration is 1 o.c. and the half-cycles adjacent to the most

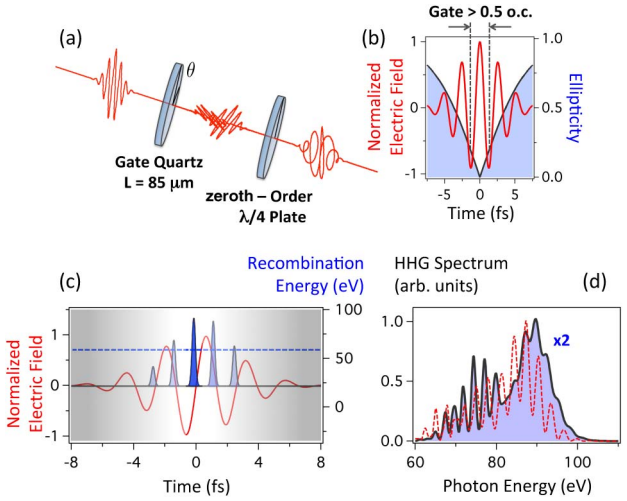

Fig. 1. (a) Schematic of PASSAGE consisting of a $L = 85$ μm quartz window and a zeroth-order $\lambda/4$ plate. The combination of these plates generates counterrotating elliptically polarized pulses. The corresponding time-dependent ellipticity is plotted in (b) for a 5 fs driving field. HHG emission occurs when the ellipticity is <0.2, creating a linear polarization gate. For PASSAGE, a polarization gate >0.5 o.c. is used to isolate the cut-off HHG spectrum. (c) Electron recombination energies for attosecond pulses driven by a 4.5 fs pulse in Ne. To isolate a SAP, a Zr filter is used to transmit photons >60 eV (blue dashed line). For linearly polarized driving fields, the Zr filter can still transmit four attosecond pulses. However, with the application of PASSAGE, the satellite pulses are greatly suppressed. (d) This is observed in the simulated HHG spectra for a linearly polarized driving field (red dashed) and PASSAGE (blue shaded). The cut-off portion of the spectrum becomes an isolated continuum with the implementation of PASSAGE.

intense half-cycle experience an ellipticity of ~0.2, leading to 1 order of magnitude reduction in their HHG contribution [11]. In this respect, PASSAGE has two clear advantages: first, using a weaker polarization gate conserves more intensity within the most intense half-cycle and accommodates access to the HHG cut-off spectrum. Second, by suppressing the emission from adjacent half-cycles, the spectral bandwidth available in the cutoff is increased.

To better understand the effect of the partial polarization gate in PASSAGE, we simulate electron recombination energies for attosecond pulses driven by a 4.5 fs driving field in neon in Fig. 1(c). To filter out the low-energy attosecond pulse train, a Zr filter is generally used as a high-pass filter at ~60 eV (blue dashed line). However, it is clear from Fig. 1(c) that the Zr filter still transmits four attosecond pulses. This can better be seen from the simulated HHG spectrum in Fig. 1(d) (see Supplement 1). For a linearly polarized field, the HHG spectrum (red dashed curve) exhibits discrete harmonics throughout its entire bandwidth. To isolate a SAP using linearly polarized light and the Zr high-pass filter, driving pulses with durations <4 fs are required. However, with the application of the weak polarization gate [gray gradient in Fig. 1(c)], the attosecond pulses adjacent to the central pulse are strongly suppressed. In the simulated HHG spectrum for PASSAGE [blue shaded curve, Fig. 1(d)], the cut-off spectrum above 80 eV turns into an isolated continuum and becomes the dominant feature in the transmitted HHG spectrum.

To isolate attosecond pulses experimentally, we begin with a carrier-envelope phase (CEP) stable, 5 fs pulse with a pulse energy of 0.8 mJ (see Supplement 1). The pulse is split with a broadband beam splitter to generate the HHG driving beam and the NIR-probe beam. The driving beam is passed through the PASSAGE optics and focused with a $f = 65$ cm spherical mirror into a 2 mm gas cell filled with either Ne or Ar gas. Attosecond pulses are isolated in Ne by using a 200 nm Zr foil as a high-pass filter for the cut-off spectrum, as described above. A typical HHG spectrum generated with a 5 fs linearly polarized driving field in Ne is shown in Fig. 2(a) (red dashed curve). Harmonic modulation is still observed in the spectrum at this driving pulse duration, indicative of satellite pulses contaminating the attosecond spectrum. However, when PASSAGE is implemented, the HHG spectrum (blue shaded curve) becomes a near perfect continuum.

Attosecond pulses are more difficult to isolate in Ar. To achieve this, we take advantage of the Cooper minimum of Ar at 50 eV [12]. In theory, if the driving pulse is short enough, harmonic emission extending from the Cooper minimum of Ar to the Al edge at 72.6 eV can be isolated to a single half-cycle of the laser field. HHG simulations suggest that the driving field would have to be <4 fs to isolate a pulse with this bandwidth. In addition, the lower ionization potential yields stricter phase-matching requirements due to additional plasma contributions [13]. As a result, the generation of isolated attosecond pulses by amplitude gating in Ar has not been observed to date. Figure 2(b) shows a typical HHG spectrum generated with a linearly polarized, 5 fs driving field in Ar (red dashed curve). The driving NIR field is filtered out using a 200 nm Al foil. Residual harmonics are clearly observed in this spectrum. However, with the implementation of

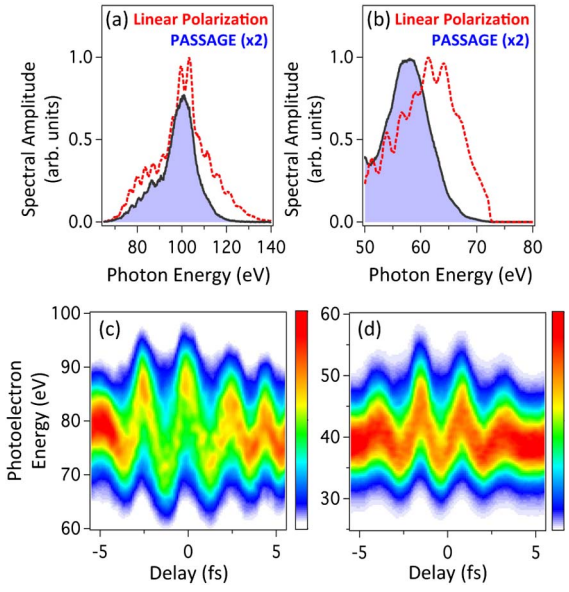

Fig. 2. Experimental SAP spectra generated using a linearly polarized driving field (red dashed curve) and PASSAGE (blue shaded curve) with (a) Ne and (b) Ar as HHG driving gases. The spectra were acquired with a driving pulse duration of 5 fs. Residual harmonic modulation is still observed in the linearly polarized case, indicative of satellite pulse contamination. The SAP spectra become nearly continuous with the implementation of PASSAGE, corresponding to the isolation of high-contrast SAPs. The isolation of the SAPs is confirmed using attosecond streaking spectroscopy. The streaking spectrograms are shown in (c) and (d) for pulses isolated in Ne and Ar, respectively.

PASSAGE, an isolated continuum extending from the Cooper minimum to the Al edge is observed.

The isolation of attosecond pulses is confirmed using the technique of attosecond streaking spectroscopy (see Supplement 1) [14]. Attosecond streaking is the conventional technique for characterizing attosecond pulses by monitoring energy-resolved photoelectrons in an XUV-pump, NIR-probe cross-correlation measurement. The streaking spectrograms recorded for attosecond pulses isolated via PASSAGE in Ne and Ar are shown in Figs. 2(c) and 2(d), respectively. The XUV and NIR fields are uniquely characterized by applying a FROG-CRAB reconstruction algorithm on the streaking spectrograms (see Supplement 1) [15]. The reconstructed attosecond pulse durations are measured to be 140 ± 10 as and 190 ± 10 as for Ne and Ar, respectively.

With the attosecond pulses well characterized, we can measure the dependence of the XUV spectrum on the CEP of the driving NIR field to better understand the mechanism giving rise to SAP production via PASSAGE. In the case of an amplitude gate, the peak photon energy of the cut-off spectrum shifts with CEP due to the changing peak amplitude of the electric field [16]. This is observed in the simulated CEP scan in Fig. 3(a) for a SAP generated from a 3.5 fs driving field in Ne (i.e., amplitude gating). The CEP dependence for PG is noticeably different. The simulated CEP scan for a SAP generated via PG with a 5 fs driving field is shown in Fig. 3(b). The CEP scan shows the evolution of the attosecond spectrum from a smooth continuum to discrete harmonics with very little center-of-energy motion in the overall spectrum. This reflects the spectrum evolving from a SAP into a double-pulse configuration [4]. From the experimental CEP scan in Fig. 3(c), a strong center-of-energy motion is observed in the attosecond spectrum as a function of CEP, suggesting that PASSAGE is an amplitude-gate-type mechanism. The difference is that the implementation of the partial polarization gate greatly relaxes the pulse duration restrictions of amplitude gating, leading to a more flexible amplitude gating scheme.

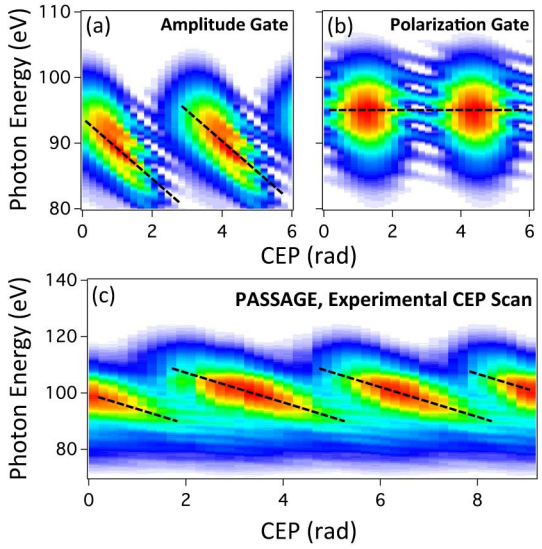

Fig. 3. (a) Simulated CEP scan for a SAP isolated using amplitude gating in Ne (3.5 fs driving field and a Zr high-pass filter). The peak position of the cut-off spectrum clearly moves with changing CEP. (b) Simulated CEP scan for a SAP isolated using PG in Ne. The center of energy of the PG spectrum is fairly insensitive to changes in the CEP. (c) The experimental CEP scan for a Ne SAP isolated using PASSAGE. The peak position of the cutoff clearly moves with changing CEP, similar to an amplitude-gate-type of mechanism.

With PASSAGE demonstrated as a robust technique for isolating SAPs, we can now compare the performance of this technique against amplitude gating and PG. The pulse energy of the SAP is measured using a calibrated XUV photodiode (Opto-diode Corp., AXUV63HS1). To optimize the photon flux, we tune either the backing HHG pressure or the focus of the driving NIR field. However, it is important to note that it is very easy to destroy the phase matching of the SAP spectrum by modifying either of these parameters due to changes in macroscopic propagation effects, resulting in the generation of a pulse train instead of a SAP. Therefore, great care is taken to preserve this CEP dependence of the SAP spectrum during the optimization process. The highest photon flux measured with PASSAGE for a SAP generated in Ar and Ne is 0.6 and 0.2 nJ, respectively (see Supplement 1). Compared to previous pulse energies measured with a PG, this represents at least 1 order of magnitude improvement in the photon flux [4]. In addition, when we implement a full polarization gate onto the pulse, the cut-off spectrum is nearly destroyed with a 95% decrease in counts above the Cooper minimum in Ar and no counts measured in Ne (see Supplement 1). When compared to using linear polarization (i.e., amplitude gate), we typically measure a reduction factor of 2–3 between linear polarization and the PASSAGE configuration. This is in line with the amplitude gate pulse energy of 0.5 nJ measured in Ne by Goulielmakis *et al.* [14].

The experimental simplicity of PASSAGE offers tremendous flexibility in the production of attosecond pulses. To tune the central energy of the attosecond pulse, one can tune the aperture of the iris, move the position of the driving laser focus, or change the HHG driving gas. Figure 4 shows six attosecond continua acquired under different PASSAGE conditions, spanning an energy range of 50–120 eV. To achieve this tunability, both Ar (red, orange, and green spectra) and Ne (blue, purple, and indigo

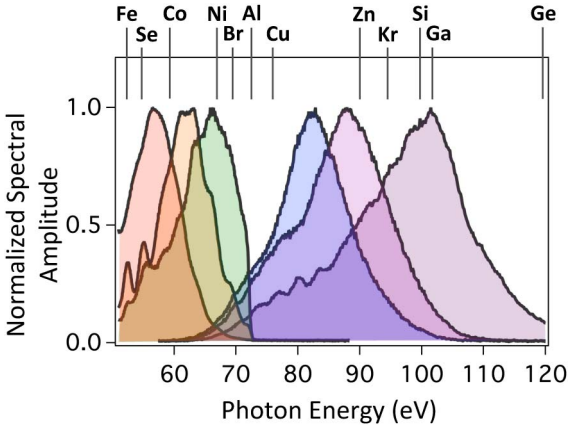

Fig. 4. Implementation of PASSAGE allows for the generation of tunable XUV continua that span the energy range of 50–120 eV. This tunability is easily achieved by a combination of adjusting the aperture of the driving beam, moving the focus, and changing the HHG driving gas. The first three spectra (red, orange, and green) were taken with Ar as a driving gas and the second three spectra (blue, purple, and indigo) were taken with Ne as a driving gas. The energy range covered by PASSAGE coincides with numerous L-, M-, and N-edge electron binding energies of chemically relevant elements.

spectra) are used as driving gases, switching between Al and Zr filters to isolate spectra below or above the Al edge at 72.6 eV, respectively. Numerous atomic binding energies exist over the spectral range offered by PASSAGE. The L-edge, M-edge, and N-edge binding energies of various elements [17] are included in Fig. 4 to represent a small subset of these possible target resonances. The attosecond spectra created through PASSAGE can be used to excite or photoionize these electrons, making it a sensitive tool for probing complex, multielectron dynamics [18].

In conclusion, we have introduced PASSAGE as a powerful technique for generating high-contrast, single attosecond pulses. The pulses can be energetically tuned between 50 and 120 eV, corresponding to an energy range that contains many chemically relevant elemental binding energies. Isolating a pulse within this regime will enable the attosecond study of multielectron dynamics in a range of interesting chemical and material systems, including halogenated hydrocarbons, organometallic compounds, and transition-metal oxides. In addition, the bandwidth and energy range of these pulses can easily be scaled with either increasing intensity or increasing wavelength. We anticipate that PASSAGE, implemented with intense, few-cycle infrared pulses [19–21], will assist in the production of broadband attosecond pulses and push the limits of attosecond pulse durations below 67 as [22]. This will enable the study of many-body electron correlation dynamics [23] and the universal response time to the removal of an electron from molecules and materials [24].

Funding. Army Research Office (ARO) (W911NF-14-1-0383); National Science Foundation (NSF) (CHE-1361226).

Acknowledgment. Johannes Hellwagner received support from the Excellence Scholarship and Opportunity Programme of ETH Zurich.

†These authors contributed equally to this work.

See Supplement 1 for supporting content.

REFERENCES

1. F. Krausz and M. Ivanov, Rev. Mod. Phys. **81**, 163 (2009).
2. E. Goulielmakis, M. Schultze, M. Hofstetter, V. S. Yakovlev, J. Gagnon, M. Uiberacker, A. L. Aquila, E. M. Gullikson, D. T. Attwood, R. Keinberger, F. Krausz, and U. Kleineberg, Science **320**, 1614 (2008).
3. P. B. Corkum, N. H. Burnett, and M. Y. Ivanov, Opt. Lett. **19**, 1870 (1994).
4. I. J. Sola, E. Mével, L. Elouga, E. Constant, V. Strelkov, L. Poletto, P. Villoresi, E. Benedetti, J.-P. Caumes, S. Stagira, C. Vozzi, G. Sansone, and M. Nisoli, Nat. Phys. **2**, 319 (2006).
5. G. Sansone, E. Benedetti, F. Calegari, C. Vozzi, L. Avaldi, R. Flammini, L. Poletto, P. Villoresi, C. Altucci, R. Velotta, S. Stagira, S. D. Silvestri, and M. Nisoli, Science **314**, 443 (2006).
6. H. Mashiko, S. Gilbertson, C. Li, S. D. Khan, M. M. Skakya, E. Moon, and Z. Chang, Phys. Rev. Lett. **100**, 103906 (2008).
7. X. Feng, S. Gilbertson, H. Mashiko, H. Wang, S. D. Khan, M. Chini, Y. Wu, K. Zhao, and Z. Chang, Phys. Rev. Lett. **103**, 183901 (2009).
8. M. J. Abel, T. Pfeifer, P. M. Nagel, W. Boutu, M. J. Bell, C. P. Steiner, D. M. Neumark, and S. R. Leone, Chem. Phys. **366**, 9 (2009).
9. F. Ferrari, F. Calegari, M. Lucchini, C. Vozzi, S. Stagira, G. Sansone, and M. Nisoli, Nat. Photonics **4**, 875 (2010).
10. T. J. Hammond, G. Brown, K. T. Kim, D. M. Velleneuve, and P. B. Corkum, Nat. Photonics **10**, 171 (2016).
11. K. S. Budil, P. Salières, A. L'Huillier, T. Ditmire, and M. D. Perry, Phys. Rev. A **48**, R3437 (1993).
12. H. J. Wörner, H. Niikura, J. B. Bertrand, P. B. Corkum, and D. M. Villeneuve, Phys. Rev. Lett. **102**, 103901 (2009).
13. M. B. Gaarde, J. L. Tate, and K. J. Schafer, J. Phys. B **41**, 132001 (2008).
14. E. Goulielmakis, V. S. Yakovlev, A. L. Cavalieri, M. Uiberacker, V. Pervak, A. Apolonski, R. Kienberger, U. Kleineberg, and F. Krausz, Science **317**, 769 (2007).
15. J. Gagnon, E. Goulielmakis, and V. S. Yakovlev, Appl. Phys. B **92**, 25 (2008).
16. C. A. Haworth, L. E. Chipperfield, J. S. Robinson, P. L. Knight, J. P. Marangos, and J. W. G. Tisch, Nat. Phys. **3**, 52 (2007).
17. A. Thomson, D. Attwood, E. Gullikson, M. Howells, K.-J. Kim, J. Kirz, J. Kortright, I. Lindau, Y. Liu, P. Pianetta, A. Robinson, J. Scofield, J. Underwood, G. Williams, and H. Winick, *X-ray Data Booklet*, 3rd ed. (Lawrence Berkeley National Laboratory, 2009).
18. Z.-H. Loh and S. R. Leone, J. Phys. Chem. Lett. **4**, 292 (2013).
19. B. E. Schmidt, N. Thiré, M. Boivin, A. Laramée, F. Poitras, G. Lebrun, T. Ozaki, H. Ibrahim, and F. Légaré, Nat. Commun. **5**, 1 (2014).
20. N. Ishii, K. Kaneshima, K. Kitano, T. Kanai, S. Watanabe, and J. Itatani, Nat. Commun. **5**, 3331 (2014).
21. Y. Yin, J. Li, X. Ren, K. Zhao, Y. Wu, E. Cunningham, and Z. Chang, Opt. Lett. **41**, 1142 (2016).
22. K. Zhao, Q. Zhang, M. Chini, Y. Wu, X. Wang, and Z. Chang, Opt. Lett. **37**, 3891 (2012).
23. A. I. Kuleff, J. Breidbach, and L. S. Cederbaum, J. Chem. Phys. **123**, 044111 (2005).
24. J. Breidbach and L. S. Cederbaum, Phys. Rev. Lett. **94**, 033901 (2005).